Journal Pre-proof

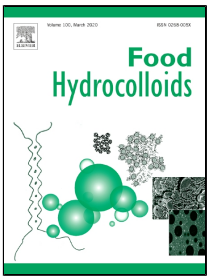

Different Aggregation States of Barley β-Glucan Molecules Affects Their Solution Behavior: A Comparative Analysis

Yang Zhao, Hui-Ming Zhou, Ze-Hua Huang, Ren-Yong Zhao

PII:	S0268-005X(19)32239-8
DOI:	https://doi.org/10.1016/j.foodhyd.2019.105543
Reference:	FOOHYD 105543
To appear in:	*Food Hydrocolloids*
Received Date:	26 September 2019
Accepted Date:	25 November 2019

Please cite this article as: Yang Zhao, Hui-Ming Zhou, Ze-Hua Huang, Ren-Yong Zhao, Different Aggregation States of Barley β-Glucan Molecules Affects Their Solution Behavior: A Comparative Analysis, *Food Hydrocolloids* (2019), https://doi.org/10.1016/j.foodhyd.2019.105543

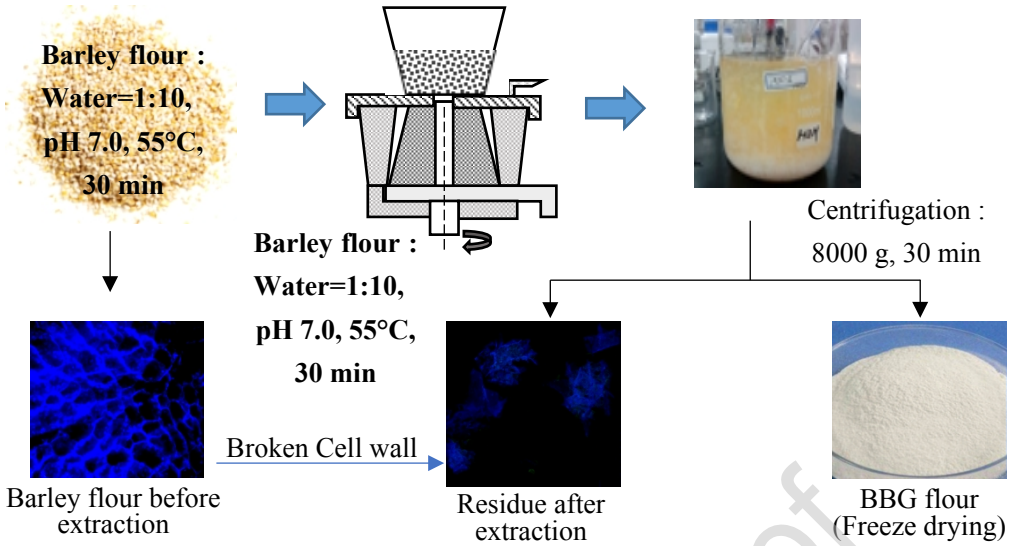

For Graphical abstract Use Only

Different Aggregation States of Barley β-Glucan Molecules Affects Their Solution Behavior: A Comparative Analysis

Yang Zhao[1], Hui-Ming Zhou[1]*, Ze-Hua Huang[1,2]*, Ren-Yong Zhao[2]

[1]State Key Laboratory of Food Science and Technology, School of Food Science and Technology, Jiangnan University, 1800 Lihu Avenue, Wuxi, Jiangsu 214122, People's Republic of China

[2] College of Food Science and Technology, Henan University of Technology, Lianhua Street, 100 Hi-tech Development Zone, Zhengzhou, Henan 450001, People's Republic of China

*Corresponding authors:

Prof. Hui-Ming Zhou

E-mail: hmzhou@jiangnan.edu.cn

Dr. Ze-Hua Huang

E-mail: huang_zehua@qq.com

Abstract: Barley β-glucan (BBG) is of admirable health advantages, the physiochemical and functional properties of BBG might be affected by its extraction process. The new high speed centrifugal-vortex extraction method was compared to a traditional method, and the extracted BBG was treated by dynamic high-pressure microfluidization (DHPM) to analysis the effect of the extraction and DHPM on molecular weight (MW), solution behavior and structural features of BBG. The new method reduced the extraction time by half, increased the yield by about 10%. The DHPM treatment made the BBG viscosity lower and the aggregation particle size distribution narrower. Although the molecular weight was reduced by DHPM treatment, the FT-IR and microstructure results showed that the exogenous physical treatment did not change the primary structure. These results indicated that the solution behavior of BBG affected by exogenous physical treatment was due to the changes of intermolecular aggregation states and high-level structure of BBG molecules.

Key words: barley β-glucan; molecular conformation; aggregation states; solution behavior; physical treatment; extraction

1. Introduction

Barley is the fourth largest grain crop in the world and is rich in barley β-glucan (BBG). BBG is a linear homopolymer linked with β-(1→3),(1→4)-D-glycosidic bonds, of which mostly two or three consecutive β-(1→4) linkages are interrupted by a single β-(1→3) linkage(Izydorczyk & Dexter, 2008). BBG has been approved by the FDA (U.S. Food and Drug Administration) and the EFSA (European Food Safety Authority)

22 to have the functional characteristics of reducing the risk of cardiovascular disease
23 (Huang, et al., 2017; C. Zielke, et al., 2017). A variety of physiological functions of
24 BBG have been reported, such as reducing postprandial blood glucose(Singhal &
25 Kaushik, 2016; S. M. Tosh, 2013), lowering serum cholesterol (M. S. Mikkelsen,
26 Jensen, & Nielsen, 2017; Wood, 2007) and promoting intestinal health(Miyamoto, et
27 al., 2018). However, while barley and BBG possess good nutritional properties, they
28 are mainly used in the elaboration of alcoholic beverages and feed industries (Mosele,
29 Motilva, & Ludwig, 2018). BBG is not commonly used in food ingredients, probably
30 because of its sensorial properties and/or limited technological (Izydorczyk, et al.,
31 2008), for example, complex BBG extraction process and higher extraction costs (Zhu,
32 Du, & Xu, 2016). Achieving the full advantages of BBG demands its easy availability
33 in great numbers and this claims the efforts on the efficient extraction of BBG.

34 BBG can be extracted in varying measures depending on the conditions used,
35 include water extraction (C. Zielke, et al., 2017), acid/alkali extraction (Kasprzak,
36 Laerke, & Knudsen, 2012), and enzymatic extraction (Lazaridou & Biliaderis, 2007).
37 In the water extraction, as the extraction temperature increases from 40 to 95 °C, the
38 recovery of β-glucan increases from 20% (Storsley, Izydorczyk, You, Biliaderis, &
39 Rossnagel, 2003) to 75% (Beer, Wood, & Weisz, 1997). However, the more starch is
40 gelatinized and dissolved at high water temperature, thus the purity tends to decrease
41 (Comino, Shelat, Collins, Lahnstein, & Gidley, 2013). The water extraction method
42 generally lasts for a long time (about 7 d)(Maheshwari, Sowrirajan, & Joseph, 2017),

leads to low intrinsic viscosity and molecular weight of BBG (Saulnier, Gévaudan, & Thibault, 1994). While the acidic or alkaline extractions are chemically treated extractions that can destroy the cell structures and promote BBG dissolution. The alkali extraction can increase the extraction levels to 86-100%, but lead to the degradation of BBG molecules (Beer, et al., 1997; Comino, et al., 2013). The enzymatic extraction, when combined with acid/alkaline extraction, shows the highest yield and highest molecular weight of β-glucan (Ahmad, Anjum, Zahoor, Nawaz, & Ahmed, 2010; Maheshwari, et al., 2017). However, the enzymatic extraction process is complex, harsh conditions and costly. These extraction methods are difficult to industrialize and to expand the scale of production, resulting in a higher cost of BBG (Maheshwari, et al., 2017). Therefore, we established a new method assisted by high speed centrifugal-vortex (HSCV) to break the cell walls of barley to accelerate the extraction of BBG.

The HSCV extraction was carried out by a colloid mill. Colloid mill equipment can work continuously, with high throughput and easy to expand production scale, making it suitable for industrial production. Colloid mill is a centrifugal device, work on the rotor-stator principle: crushing grinding relies on the toothed bevel disc (rotor and stator) relative motion. The resulting high-frequency vibrations and high-speed vortex squeeze applied to the process liquid and disrupt cell walls of barley in the fluid, thereby improving the extraction efficiency of BBG.

The admirable health advantages of BBG have been proved in many studies (Makela, Sontag-Strohm, et al., 2017; Rieder, Knutsen, & Ballance, 2017; Singhal, et

al., 2016), the beneficial of BBG shows molecular weight and fine structure-dependent (Rieder, Grimmer, Kolset, Michaelsen, & Knutsen, 2011; Skau-Mikkelsen, Jespersen, Mehlsen, Engelsen, & Frokiaer, 2014). It is noteworthy to note that the molecular weight, solution behavior and structural features of BBG are significantly affected by the extraction method. Therefore, this study compared the basic properties of BBG extracted by traditional water extraction and HSCV extraction. Meanwhile, the obtained BBG was physically modified by the dynamic high-pressure microfluidization (DHPM) treatment. The DSC, TGA, FI-IR, X-Ray, rheology, particle size analysis, SEM and other analytical methods were used to analyze rheology, solution aggregation state and molecular structure of BBG, aimed to find out the reasons for the impacts of different physical treatment processes on the properties of BBG solution.

2. Materials and Methods

2.1 Materials

Barley flour (BF) was purchased from *Dafeng Deren Mairen Factory* (harvested in 2014, Suonong-16), particle size 80-100 mesh (13.8% moisture (AACC 44-15.02), 11.3% protein (AACC 46-30.01), 67.9% starch (hydrolytic method and titrated by $Na_2S_2O_3$), 2.8% β-glucan (AACC Method 32-23), and 0.88% ash (AACC Method 08-01)). Pancreatin from hog pancreas was purchased from Sigma-Aldrich Shanghai Trading Co., Ltd. (Shanghai, China). Thermostable α-amylase was purchased from Jiangsu Ruiyang Biotech Co., Ltd. (Wuxi, China). All other reagents used were of analytical grade, and deionized water was used throughout unless otherwise stated.

85 2.2 Extraction of Barley β-glucan

86 BF was pretreated with 85% ethanol at a BF-ethanol ratio of 1:10 (100 g:1 L) and
87 refluxed at 85 °C for 2 h to inactivate endogenous enzymes. Barley β-glucan (BBG)
88 was extracted by two methods. For comparison, we chose a mild extraction method that
89 minimizes the degradation of BBG molecules as the traditional extraction method (TE-
90 method) (Huang, et al., 2017). In the TE-method BBG was extracted at pH of 7.0,
91 stirring and leaching at 55 °C for 2 h at a BF-water ratio of 1:10 (100 g:1 L). The second
92 method was the high-speed centrifugal vortex method (HSCV-method) to assist in the
93 extraction of BBG. The HSCV-method was achieved with a colloid mill (JMFB-80,
94 Shanghai Kelao Mechanical Equipment Co., Ltd., Shanghai, China) for 30 min. The
95 colloid mill speed is 8000 r/min and the stator and rotor clearance are set to 1.5 mm.
96 The pH, temperature, and solid-liquid ratio were the same as TE-method. The extracts
97 obtained by the above two methods were centrifuged at 8000 g for 15 min, and the
98 supernatant was named as BBG extract. The contaminating starch of the BBG extract
99 was hydrolyzed by thermostable α-amylase (preheated to 95 °C and kept for 30 min) at
100 10 units/mL, pH 6.5, and temperature of 95 °C for 30 min, cool to room temperature,
101 known as the Enzymatic solution I. The contaminating proteins of the Enzymatic
102 solution I were removed by pancreatin from hog pancreas at 0.05 mg/mL, pH 4.5, and
103 40 °C for 3 h, known as the Enzymatic solution Ⅱ. Enzymatic solution II was
104 centrifuged at 8000 g for 15 min, the supernatant was adjusted to pH 7.0, and was
105 rotovapped to 1/3 of the original volume at 55 °C. After centrifugation at 8000 g for 15

106 min, BBG was obtained by precipitating with 95% (v/v) ethanol, and then the sediments
107 were washed twice with 95% (v/v) ethanol and freeze-dried. The recovery rate of BBG
108 can be calculated as the following equation: BBG recovery rate =
109 $\frac{\text{BBG extracted (mg)}}{\text{BBG content in barley flour (mg)}} \times 100\%$.

110 2.3 Fluorescence microscopy analysis

111 The effect of two different extraction methods on the dissolution of glucan in
112 barley kernels was studied by fluorescence microscopy (Sikora, Tosh, Brummer, &
113 Olsson, 2013; Yu, Zhou, Zhu, Guo, & Peng, 2019). 50 μL of FITC (0.25%, w/v,
114 preferentially staining starch) and calcofluor white (0.01%, v/v, preferentially staining
115 BBG) were sequentially added to the barley flour residue after extraction and stain for
116 2 min. The stained samples were observed under a fluorescence microscope (Axio Vert
117 A1, Carl Zeiss Microscopy GmbH, Jena, Germany) using a light emitting diode (LED)
118 filter set. The excitation/emission wavelengths were 488/518 nm for FITC and 410/455
119 for calcofluor white. Samples were viewed with a 10× objective in an AxioCam MRC
120 Zeiss camera and analyzed by Zen 2012 software.

121 2.4 Dynamic high pressure micro-fluidization treatment of BBG

122 Accurately weighed 10 g of BBG extracted by the two methods, and added it to 1
123 L of water, respectively. Heated the mixture to 80 °C in a water bath and oscillate
124 intermittently to completely dissolve barley β-glucan. The obtained 1% BBG solutions
125 were homogenized 3 times at 80 MPa in a dynamic high pressure micro-fluidizer (M-
126 700 Series, Microfluidics Corp., Westwood, MA 02090, USA). After DHPM treatment,

127 BBG was precipitated with 95% ethanol, washed and freeze-dried.

128 2.5 Determination of BBG content and purity

129 The purity of BBG was determined by the Congo red method (Kupetz, et al., 2016).
130 β-glucan and Congo red dye can specifically bind, and the binding product has strong
131 light absorption properties at 550 nm. First, prepare a BBG standard solution with a
132 concentration of 0.1 mg / mL and dilute to a series of concentration gradients of 0.01,
133 0.02, 0.04, 0.06, 0.08, and 0.1 mg/mL, respectively. Pipetted 1.0 ml of each
134 concentration of BBG standard solution into 4.0 mL Congo red solution and mix well.
135 The mixtures were protected from light at 25 ° C for 10 min. Pipetted 200 μL of each
136 mixture into a 96-well plate and measure the absorbance of the solution at 550 nm using
137 a Bio-Tek microplate reader (EPOCH2, BioTek Instruments, Inc., Winooski, VT, USA)
138 and draw a standard curve. The absorbance of the BBG sample solution was determined
139 as described above, and the BBG content in the sample was calculated from the standard
140 curve. The purity of BBG can be calculated as the following equation: $\text{BBG purity} =$
141 $\frac{\text{BBG content calculated (mg)}}{\text{BBG sample (mg)}} \times 100\%$.

142 2.6 Determination of molecular weight of BBG

143 The glucan was measured by multi-angle laser light scattering (MALLS) high
144 performance liquid chromatography (HPLC) (Storsley, et al., 2003). The mobile phase
145 was 0.1 mol/L $NaNO_3$ containing 0.02% NaN_3, the flow rate was 0.8 ml/min, the
146 injection volume is 10 μL, and the TSK gel 4000 analytical column (Tosoh Biosep,
147 Tokyo, Japan) was used, and the temperature of the column oven was 30 °C. The

148 Waters Alliance HPLC system (Waters Corporation, Milford Massachusetts, USA) is
149 coupled with Dawn Heleos II multi-angle laser light scattering (Wyatt Technology,
150 Germany) and a Waters Acquity refractive index (RI) detector for quantitative detection.
151 The results were analyzed by ASTRA version 5.3.4.20 (Wyatt Technology, Germany).

152 2.7 Rheological Measurements

153 Accurately weighed 300 mg of different BBG samples, dissolved in 10 mL of
154 water, and shook in a water bath at 80 °C until the BBG was completely dissolved. A
155 proper amount of the 3% BBG solution was loaded in the 40 mm plate and plate
156 geometry, the temperature was set at 25 °C, the gap was 1000 μm, and the soak time
157 was 300 s. Two types of rheological properties of the 3% solution of different BBG
158 samples were determined by a DHR3 rheometer (TA Instruments, West Sussex, U.K.):
159 (1) flow behavior was carried out at shear rates between 0.1 and 300 s^{-1}; (2) oscillation
160 frequency sweep programs were frequency from 0.1 to 10 Hz at the linear viscoelastic
161 regime. All the measurements were performed in triplicate, and a few drops of paraffin
162 oil were added to the edge of the samples to prevent water evaporation.

163 2.8. Particle size distribution determination

164 The particle size of the BBG was measured by NanoBrook Omni (Brookhaven
165 Instruments Corp. USA) equipped with an optical pump semiconductor laser (35 mW,
166 640 nm wavelength) (Ningtyas, Bhandari, Bansal, & Prakash, 2018). The BBG sample
167 was dissolved in distilled water at room temperature and shaken until the BBG was
168 completely dissolved. The BBG solution was added to a plastic cuvette and measured

169 at a 90° scattering angle of 25°C.

170 2.9 Scanning electron microscope

171 The surface morphology of BBG was visualized with a scanning electron
172 microscope (S-4300, Hitachi, Tokyo, Japan) at an acceleration voltage of 5.0 kV. In
173 order to obtain a clear SEM image, dried BBG powder samples of different treatments
174 were evenly spread onto the conductive tape and pasted onto the sample stage and
175 sputter-coated with gold (Sputter coater E-1030, Hitachi, Tokyo, Japan) (Sullivan, et
176 al., 2009).

177 2.10 Thermogravimetric analysis

178 The thermal stability of BBG was determined by thermogravimetric analysis
179 (TGA/SDTA 851e, Mettler Toledo Corp., Zurich, Switzerland) (Nie, et al., 2019).
180 Different BBG powder samples of approximate 3 mg were weighed into 70 μL ceramic
181 pans, heated from 30 to 600 °C at a heating rate of 10 °C/min. The nitrogen flow rate
182 was 50 mL/min. The thermogravimetric curve was analyzed by STARe evaluation
183 software (Mettler Toledo Corp., Zurich, Switzerland).

184 2.11 X-ray diffraction analysis

185 X-ray diffraction analysis (XRD) of different BBG powder samples were carried
186 out by an X-ray diffractometer equipped with a Cu, standard ceramic sealed tube and
187 LYNXEYE XE-T detector (D2 PHASER, Bruker, Karlsruhe, Germany) (Miller &
188 Fulcher, 1994).The samples were evenly spread into the XRD Specimen Holders,
189 gently compacted and smoothed. Measurements were operating at 30 kV and 10 mA.

The samples were analyzed in an angular (2θ) range from 4° to 45° in 0.04° steps. Data interpretation was done using JADE 6.

2.12 Fourier transform infrared (FT-IR) analysis

FT-IR spectroscopy was performed on a Nicolet iS10 FT-IR spectrometer (ThermoFisher Scientific, Waltham, MA USA). BBG powder (1 mg) was thoroughly ground with 100 mg potassium bromide (KBr) powder in an agate mortar(Mette S. Mikkelsen, et al., 2010). The mixture was then pressed at approximately 10 Mpa in a metal container to tablet the KBr disc specimen. The spectrum was collected with 64 scans at a resolution of 4 cm^{-1} and the spectral was in the range of 4000 to 400 cm^{-1}. Before each sample measurement, the background spectrum was scanned at room temperature using blank potassium bromide tablets and the sample scanning and background scanning methods were the same as in the environment. The spectroscopy of the BBG samples was analyzed by Omnic software (version 9.3.30, Thermo Nicolet Inc.).

2.13 Statistical Analysis.

All samples were independently prepared and measured in triplicates. Significant differences of evaluated parameters among different samples were performed using an analysis of variance (ANOVA) procedure with SPSS statistical software (version 22.0, SPSS, Inc., Chicago, IL, U.S.A.). The significance test level is $p < 0.05$.

3 Results and Discussion

3.1 The basic properties of TE-extraction and HSCV-extraction of BBG

211 Table 1. Basic characteristics of barley β-glucan extracted and treated differently. In the table,
212 TE stands for the traditional extraction; HSCV for the high-speed centrifugal vortex extraction;
213 DHPM for dynamic high-pressure microfluidization treatment of TE and HSCV extraction,
214 respectively. Data with different letters in the same column are significantly different ($p < 0.05$).

BBG Sample	Relative molecular mass ($\times 10^6$)	Purity (%)	Recovery rate (%)
TE-extraction	2.19 ± 0.20^{a}	89.4 ± 1.7^{ab}	67.7 ± 1.2^{b}
HSCV- extraction	1.38 ± 0.05^{b}	84.7 ± 2.3^{b}	79.4 ± 1.7^{a}
DHPM (TE-extraction)	0.97 ± 0.03^{c}	90.0 ± 2.1^{a}	/
DHPM (HSCV- extraction)	0.70 ± 0.01^{c}	86.4 ± 1.1^{ab}	/

215 It can be seen from Table 1 that the relative molecular mass and purity of the BBG
216 obtained by the traditional extraction method was greater than the relative molecular
217 mass of the BBG obtained by the HSCV method. The result was in agreement with
218 previous studies (Ahmad, et al., 2010; Beer, et al., 1997; Comino, et al., 2013;
219 Maheshwari, et al., 2017; Saulnier, et al., 1994), which indicated that the molecular
220 weight of BBG obtained by different extraction methods was different. Perhaps it was
221 caused by the difference in the molecular degradation and/or the entanglement state of
222 BBG molecules in different extraction processes. However, the purity of the two
223 methods differs by about 4.7% and the extraction rate of BBG obtained by HSCV
224 extraction was increased by about 11.7%.

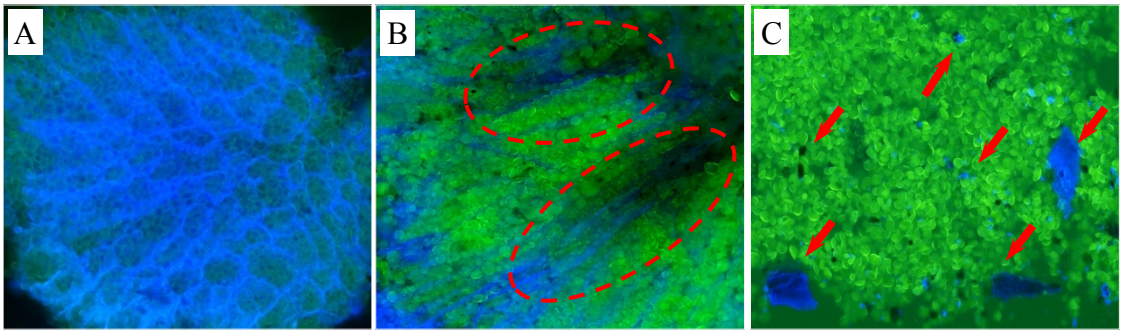

Figure 1. Fluorescence micrograph of the residue after extraction of barley flour. BBG is dyed blue by calcofluor white and starch granules are dyed green by FITC. Among these pictures, A is the fluorescence micrograph of the original barley flour, B is the fluorescence micrograph of the residue after 2 h of hot water extraction at 55 °C, and C is the fluorescence micrograph of the residue after high-speed centrifugal vortex breaking cell wall extraction for 30 min.

In order to increase the dissolution rate of BBG, it was an effective method to expand the contact area of BBG in the solvent. BBG was mainly distributed in the cell wall of barley endosperm containing starch granules (Figure 1A), which was consistent with the results of Miller et al. (Miller, et al., 1994). Comparing Fig. 1B with Figure 1C, it can be found that HSCV extraction could strongly pulverize the cell wall structure of barley endosperm, disperse the cell wall into fine particles, increase the contact area between the cell wall and the extraction solvent, and thus made the BBG in the cell wall more soluble.

Dynamic high-pressure microfluidization (DHPM) is a high-pressure technology that integrates multi-unit operations such as mixing, crushing, homogenization and transportation. DHPM can affect the microstructure of materials by high-speed impact, high-speed shear, instantaneous pressure release, and hole explosion. It is a potential

emerging technology for the physical modification of polysaccharides. After the extracted BBG sample was treated by DHPM, the relative molecular mass and the radius of rotation of BBG decreased (Table 1). These results show that different extraction methods and physical treatment methods have significant effects on the molecular weight, molecular structure and physical properties of BBG.

3.2 Effect of the extraction process and physical modification on the solution behavior of BBG

3.2.1 Rheological properties of BBG

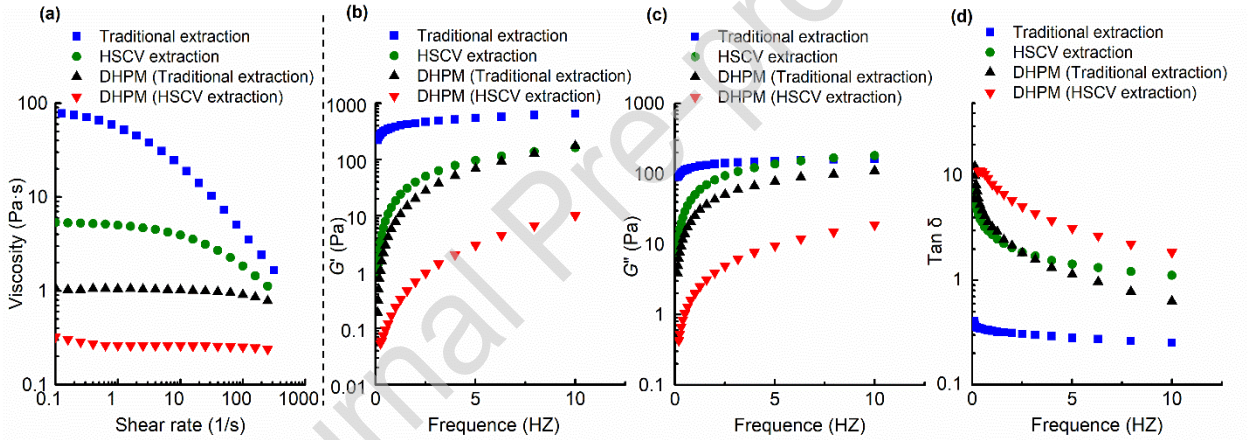

Figure 2. Rheological properties of barley beta-glucan. The concentration of the samples was 3%. In the figure, (a) is the viscosity curve of BBG solution; (b)-(d) is *G*', *G*''and tan δ of oscillatory (dynamic) frequency sweep test of BBG solution, respectively.

The viscosity of BBG was considered to be a vital factor for its functional properties (Makela, Maina, Vikgren, & Sontag-Strohm, 2017). It is worthy to note in figure 1a that the raw BBG solutions without HSCV extraction and DHPM treatment were showed more pronounced shear thinning flow behavior. This indicated that the process of HSCV extraction significantly affected the rheological properties of the BBG

solution, which was consistent with the results of Aktas-Akyildiz et al. (Aktas-Akyildiz, et al., 2018). As reported by Tosh et al., the differences in response to shear of polymers are caused by very transient entanglement, such as less transitory intermolecular hydrogen bonds, relatively stable regions formed by multiple hydrogen bonds, and aggregation of gel particles, and the increase in G' at tan $\delta>1$ is the result of polymer entanglement in the sample system (Susan M. Tosh, Wood, Wang, & Weisz, 2004). Figure 2 b and c showed that the G' and G'' of the traditional-method extracted BBG were the highest and the G' and G'' of the HSCV-extracted BBG treated by DHPM was the lowest. At frequencies below 5 Hz, the G' and G'' were increased significantly of all the samples except the BBG extracted by the traditional method. While, over the entire frequency range (0.1-10 Hz), the tan δ of the BBG extracted by the traditional method is less than 1. The changes in rheological behavior of the BBG solutions might be due to conformational changes of the BBG molecules from a random-coil type to a more ordered form, which might be related to interchain aggregation (Lazaridou, Biliaderis, Micha-Screttas, & Steele, 2004). According to a popular model, the aggregation of BBG was caused by the interconnection of more than three consecutive β-(1→4)-linked D-glucopyranosyl units of cellulose-like structure (Fincher & Stone, 1986). BBG linear chains would assemble through hydrogen bonds between these cellulose-like regions, and the microgel appeared a somewhat fringed micelle structure (Claudia Zielke, Lu, & Nilsson, 2019). Thus, it should be noted that the conformation of the BBG molecules and the intermolecular entanglements play an important role in

281 the rheological properties.

282 **3.2.2 Particle size distribution of BBG in solution**

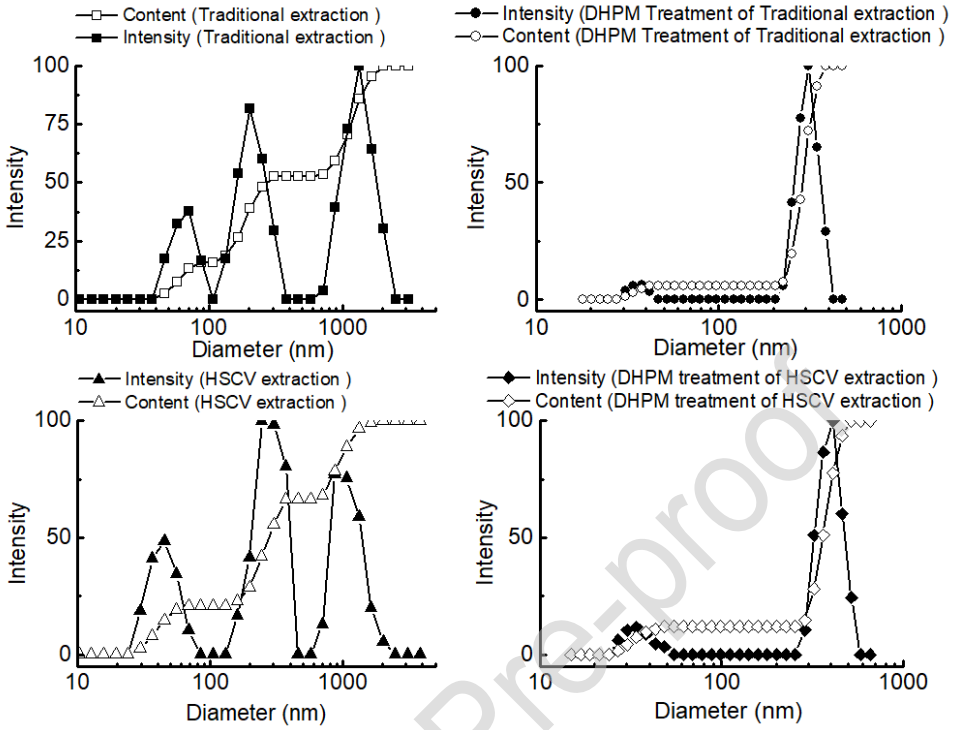

283

284 Figure 3. Particle size distribution of barley beta-glucan.

285 The conformation of BBG usually appears as a random coil, single helix, multi-
286 helical structure, and is remarkably affected by intermolecular forces, temperature and
287 solvent (Wang, et al., 2017). Different extraction processes would cause changes in the
288 factors that affect the BBG conformation, so that BBG exhibits different aggregation
289 states. The particle size distribution is one of the indexes for the state of aggregation of
290 BBG. It can be seen from Figure 3 that the BBG extracted by the two methods had three
291 different polydisperse systems. This polydisperse system was similar to the solution
292 aggregation model of Korompokis et al., who reported that there were primary
293 aggregates, secondary supramolecular aggregate structures (microgel structures), and

294 high density secondary aggregates in oat beta-glucan solution (Korompokis, Nilsson,
295 & Zielke, 2018). The proportion (about 30%) of BBG particles with large diameter
296 (500-1000 nm) extracted by HSCV was smaller than that extracted by traditional
297 methods (about 50%). This might be that the conformation of the BBG was changed
298 during the HSCV extraction process. This change inturns affected the aggregation of
299 BBG in solution, which might be the reason why the shear effect changed the
300 rheological properties of BBG.

301 The BBG obtained by two different extraction methods were treated by DHPM
302 respectively. After DHPM treatment, the particle size was mainly distributed at about
303 300 nm, indicated that the DHPM treatment made the particle size distribution of BBG
304 uniform. It is well known that the nutritional function of β-glucan is determined by
305 physicochemical and structural properties (Korompokis, et al., 2018). One of the most
306 commonly discussed mechanisms is that β-glucan can form a gel in solution, increasing
307 the viscosity of the chyme and thus exerting physiological functions (Grundy, et al.,
308 2017). According to Grimm et al., the particle weight of β-(1,3)(1,4)-glucan strongly
309 depends on the external forces (Grimm, Krüger, & Burchard, 1995). The particle size
310 distribution and aggregation state of BBG are the important factors affecting the
311 solution viscosity and gel network structure, and thus affecting the functional properties
312 of β-glucan. It was found that the gelation process of cereal beta-glucan (BBG, oat β-
313 glucan) depend on the molar mass and aggregation state of the beta-glucan molecules
314 (Makela, Maina, et al., 2017). Therefore, the behavior of BBG in solution was the final

result of a series of effects during extraction and processing.

3.3 Effect of the extraction process and physical modification on the molecular structure of BBG

According to the DTGA curve of BBG, there were three peaks during the temperature rise from 30 °C to 600 °C, showed that BBG thermal decomposition has three stages. According to Zamora et al. (Zamora, et al., 2002), these three stages corresponded to the loss process of water (30-150 °C), the preliminary thermal decomposition process (250-350 °C, polysaccharide long-chain dehydration reaction, scissions of C–O bonds), as well as char-forming reactions of the polymer molecules (350-600 °C). As can be seen from Figure 4A, the mass loss trend of the BBG obtained by the two different extraction methods was the same when the temperature ranging from 150 to 350 °C. It was indicated that different extraction methods do not affect the water evaporation and preliminary thermal decomposition process of BBG. When the temperature was above 350 °C, the BBG molecules completely depolymerize and begin to carbonize (Zamora, et al., 2002). The pyrolysis temperature of the BBG extracted by the traditional method was higher than that of the BBG extracted by HSCV method (as shown in zone 3 of Figure 4B). The thermal stability of the BBG extracted by the HSCV method was lowered. However, different from raw BBG samples extracted by the two extraction methods, after the DHPM treatment, there were only two thermal decomposition process; moreover, the thermal decomposition temperature of the HSCV extraction of BBG was slightly lowered (zone 3 in figure 4B). Why the BBG

decomposition process differences? We thought this might be due to the changes in the aggregation state of BBG molecules.

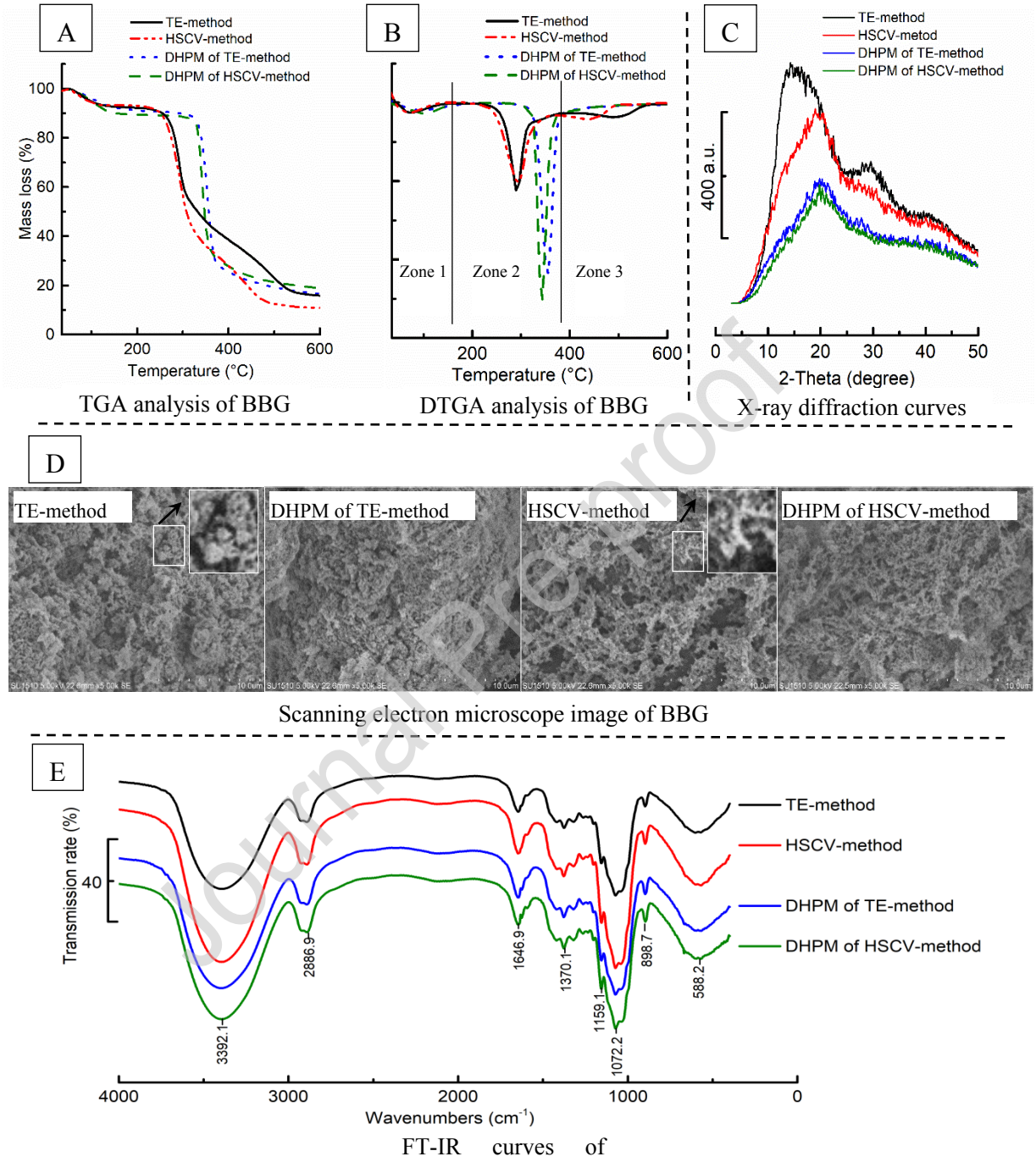

Figure 4. Structural analysis of BBG molecules. Figure 4A-4E are respectively TGA analysis of BBG; DTGA analysis of BBG; X-ray diffraction curves of BBG; scanning electron microscope image of BBG; FT-IR curves of BBG.

342 The microscopic photograph of the BBG extracted by the traditional method (TE-
343 method) could be observed a lot of cluster-like structures like knotted "wool clusters"
344 (Figure 4D). These small clusters had a dense surface and no fine pore structure. This
345 dense microstructure might indicate the existed of high-strength topological
346 entanglement and/or intermolecular aggregation (Karimi, Azizi, & Xu, 2019). The
347 photomicrographs of the BBG extracted by the HSCV method showed a coral-like
348 branched structure. These microscopic features with a large number of small pores were
349 expected to produce greater adsorption capacity and better water holding capacity. The
350 molecular weight of BBG extracted by the HSCV method was smaller than that of TE-
351 method. It has been reported that samples with a lower molecular weight are prone to
352 aggregation (Ren, Ellis, Ross-Murphy, Wang, & Wood, 2003). Whereas when the
353 molecular weight increased, the size of the aggregates is significantly increased (Wu,
354 et al., 2006). Therefore, BBG extracted by the TE-method formed a large cluster-like
355 aggregate structure, supporting results shown previously that the BBG extracted by TE-
356 method with larger particle size. Furthermore, after DHPM treatment, the
357 photomicrographs exhibited more porous and spongy structure than before, appeared
358 as complex networks. At the same time, the cluster-like structure of BBG extracted by
359 the TE-method suggested a high entanglements structure of the BBG molecular, and
360 this denser state required higher thermal decomposition temperature. However, in the
361 coral-like branch structure of the BBG extracted by HSCV method, the fine branches
362 were more easily depolymerized and fractured, thus the degradation occurred at lower

363 temperatures, but the degradation process was prolonged. Such aggregation state
364 changes might be one explanation of the differences in the BBG decomposition process
365 obtained by different extraction processes in thermogravimetric analysis (Figure 4B).

366 An investigation based on X-ray diffraction has been shown BBG is crystallized
367 in the same way as lichenan (Tvaroska, Ogawa, Deslandes, & Marchessault, 1983). By
368 observing the X-ray curves of different types of BBG, it was found that the peak area
369 and peak width of BBG extracted by the TE-method were larger than those of BBG
370 extracted by the HSCV method. A larger peak width means that there are multiple
371 crystal-like forms and lattice types in the crystalline portion of the sample. At the same
372 time, the BBG extracted by TE-method had a larger molecular mass and was not easy
373 to form a gel network structure (Ren, et al., 2003), but could form a larger size
374 aggregates (Wu, et al., 2006), so that resulted in the presence of both microgels and
375 intermolecular macromolecular entanglements in BBG samples. In other words, in the
376 BBG samples, the relatively regular crystalline and amorphous forms exist in the same
377 system.

378 The primary structure and conformation of β-glucan play an important role in its
379 biological activity. For example, the antitumor activity of a lentinan consisting of β-
380 (1→3) linkages was markedly reduced when the conformation was destroyed (Zhang,
381 Li, Xu, & Zeng, 2005). Fourier transform infrared spectroscopy (FT-IR) can monitor
382 the structural changes in biopolymers for structural analysis of polysaccharides to
383 determine the chemical functional groups and intermolecular chemical bonds in

384 samples (Ahmad, et al., 2010; Hematian Sourki, Koocheki, & Elahi, 2017). It could be
385 observed by the FT-IR spectrum from Figure 4E that it was a characteristic absorption
386 peak of the β-glycosidic bond at 896 cm^{-1}, which was consistent with the structure of
387 β-glucan. Comparing the FT-IR curves of the different BBG samples in Figure 4E, it
388 was found that the characteristic absorption peaks were consistent in the infrared
389 spectra of all BBG samples, indicating that the primary structure of the BBG molecules
390 was not altered. From the above analysis, it concluded that after different extraction
391 methods and high-speed vortex centrifugal shearing treatment, the molecular weight
392 and molecular chain conformation of BBG were changed, resulting in different
393 polymerization states, and it appeared as a change in microscopic morphology and X-
394 ray diffraction results. The different ways in which these BBG molecular chains were
395 entangled and agglomerated in turn lead to changes in the TGA thermal stability and
396 rheological properties of BBG.

397 **4. Conclusions**

398 This study compared the new high speed centrifugal-vortex extraction method to
399 the traditional method. Then the extracted BBG was treated by dynamic high-pressure
400 microfluidization (DHPM). The molecular weight, solution behavior and structural
401 features of BBG were analyzed. The new method reduced the extraction time by half,
402 increased the yield by 13.8%. After DHPM treatment, the particle size distribution of
403 the BBG solution was more uniform, and the solution showed a stronger fluid property
404 and lower viscosity. Although the molecular weight was reduced by DHPM treatment,

the FT-IR and microstructure results showed that the exogenous physical treatment did not change the primary structure but changed the intermolecular aggregation state of the BBG molecules. These results indicated that the high-level structure and aggregation state of BBG molecules was one of the noticeable reasons why the extraction and physical treatment that affect their solution behavior.

Conflicts of interest

The authors declare that they have no conflict of interest.

Acknowledgment

This work was financially supported by the National Natural Science Foundation of China (Grant 31772006), the Postgraduate Research & Practice Innovation Program of Jiangsu Provence (Grant KYCX17_1412)

References

Ahmad, A., Anjum, F. M., Zahoor, T., Nawaz, H., & Ahmed, Z. (2010). Extraction and characterization of β-d-glucan from oat for industrial utilization. *International Journal of Biological Macromolecules, 46*(3), 304-309.

Aktas-Akyildiz, E., Sibakov, J., Nappa, M., Hytonen, E., Koksel, H., & Poutanen, K. (2018). Extraction of soluble beta-glucan from oat and barley fractions: Process efficiency and dispersion stability. *Journal of Cereal Science, 81*, 60-68.

Beer, M. U., Wood, P. J., & Weisz, J. (1997). Molecular weight distribution and (1->3)(1->4)-beta-D-glucan content of consecutive extracts of various oat and barley cultivars. *Cereal Chemistry, 74*(4), 476-480.

Comino, P., Shelat, K., Collins, H., Lahnstein, J., & Gidley, M. J. (2013). Separation and Purification of Soluble Polymers and Cell Wall Fractions from Wheat, Rye and Hull less Barley Endosperm Flours for Structure-Nutrition Studies. *Journal of Agricultural and Food Chemistry, 61*(49), 12111-12122.

Fincher, G. B., & Stone, B. A. (1986). *Cell walls and their components in cereal grain technology. In Y. Pomeraz (Ed.)*: American Association of Cereal Chemists.

Grimm, A., Krüger, E., & Burchard, W. (1995). Solution properties of β-D-(1, 3)(1, 4)-glucan isolated from beer. *Carbohydrate Polymers, 27*(3), 205-214.

Grundy, M. M. L., Quint, J., Rieder, A., Ballance, S., Dreiss, C. A., Butterworth, P. J., & Ellis, P. R. (2017). Impact of hydrothermal and mechanical processing on dissolution kinetics and rheology of oat β-glucan. *Carbohydrate Polymers, 166*, 387-397.

Hematian Sourki, A., Koocheki, A., & Elahi, M. (2017). Ultrasound-assisted extraction of β-d-glucan from hull-less barley: Assessment of physicochemical and functional properties. *International Journal of Biological Macromolecules, 95*, 462-475.

Huang, Z. H., Zhao, Y., Zhu, K. X., Guo, X. N., Peng, W., & Zhou, H. M. (2017). Effect of Barley beta-Glucan on the Gluten Polymerization Process in Dough during Heat Treatment. *Journal of Agricultural and Food Chemistry, 65*(29), 6063-6069.

Izydorczyk, M. S., & Dexter, J. E. (2008). Barley β-glucans and arabinoxylans: Molecular structure, physicochemical properties, and uses in food products–a Review. *Food Research International, 41*(9), 850-868.

Karimi, R., Azizi, M. H., & Xu, Q. (2019). Effect of different enzymatic extractions on molecular weight distribution, rheological and microstructural properties of barley bran β-glucan. *International Journal of Biological Macromolecules, 126*, 298-309.

Kasprzak, M. M., Laerke, H. N., & Knudsen, K. E. B. (2012). Changes in Molecular Characteristics of Cereal Carbohydrates after Processing and Digestion. *International journal of molecular sciences, 13*(12), 16833-16852.

Korompokis, K., Nilsson, L., & Zielke, C. (2018). The effect of in vitro gastrointestinal

conditions on the structure and conformation of oat β-glucan. *Food Hydrocolloids, 77*, 659-668.

Kupetz, M., Aumer, J., Harms, D., Zarnkow, M., Sacher, B., & Becker, T. (2016). High-throughput β-glucan analyses and their relationship with beer filterability. *European Food Research and Technology, 243*(2), 341-351.

Lazaridou, A., & Biliaderis, C. G. (2007). Molecular aspects of cereal beta-glucan functionality: Physical properties, technological applications and physiological effects. *Journal of Cereal Science, 46*(2), 101-118.

Lazaridou, A., Biliaderis, C. G., Micha-Screttas, M., & Steele, B. R. (2004). A comparative study on structure − function relations of mixed-linkage (1→3), (1→4) linear β-d-glucans. *Food Hydrocolloids, 18*(5), 837-855.

Maheshwari, G., Sowrirajan, S., & Joseph, B. (2017). Extraction and Isolation of beta-Glucan from Grain Sources-A Review. *Journal of Food Science, 82*(7), 1535-1545.

Makela, N., Maina, N. H., Vikgren, P., & Sontag-Strohm, T. (2017). Gelation of cereal beta-glucan at low concentrations. *Food Hydrocolloids, 73*, 60-66.

Makela, N., Sontag-Strohm, T., Schiehser, S., Potthast, A., Maaheimo, H., & Maina, N. H. (2017). Reaction pathways during oxidation of cereal beta-glucans. *Carbohydrate Polymers, 157*, 1769-1776.

Mikkelsen, M. S., Jensen, M. G., & Nielsen, T. S. (2017). Barley beta-glucans varying in molecular mass and oligomer structure affect cecal fermentation and microbial composition but not blood lipid profiles in hypercholesterolemic rats. *Food Function, 8*(12), 4723-4732.

Mikkelsen, M. S., Jespersen, B. M., Møller, B. L., Lærke, H. N., Larsen, F. H., & Engelsen, S. B. (2010). Comparative spectroscopic and rheological studies on crude and purified soluble barley and oat β-glucan preparations. *Food Research International, 43*(10), 2417-2424.

Miller, S. S., & Fulcher, R. G. (1994). Distribution of (1-]3), (1-]4)-Beta-D-Glucan in Kernels of Oats and Barley Using Microspectrofluorometry. *Cereal Chemistry, 71*(1), 64-68.

Miyamoto, J., Watanabe, K., Taira, S., Kasubuchi, M., Li, X., Irie, J., Itoh, H., & Kimura, I. (2018). Barley beta-glucan improves metabolic condition via short-chain fatty acids produced by gut microbial fermentation in high fat diet fed mice. *PLoS One, 13*(4), e0196579.

Mosele, J. I., Motilva, M.-J., & Ludwig, I. A. (2018). Beta-Glucan and Phenolic Compounds: Their Concentration and Behavior during in Vitro Gastrointestinal Digestion and Colonic Fermentation of Different Barley-Based Food Products. *Journal of Agricultural and Food Chemistry, 66*(34), 8966-8975.

Nie, Y., Jin, Y., Deng, C., Xu, L., Yu, M., Yang, W., Li, B., & Zhao, R. (2019). Rheological and microstructural properties of wheat dough supplemented with Flammulina velutipes (mushroom) powder and soluble polysaccharides. *Cyta-Journal of Food, 17*(1), 455-462.

Ningtyas, D. W., Bhandari, B., Bansal, N., & Prakash, S. (2018). Texture and lubrication properties of functional cream cheese: Effect of beta-glucan and phytosterol. *J Texture Stud, 49*(1), 11-22.

Ren, Y., Ellis, P. R., Ross-Murphy, S. B., Wang, Q., & Wood, P. J. (2003). Dilute and semi-dilute solution properties of (1→3), (1→4)- β -d-glucan, the endosperm cell wall polysaccharide of oats (Avena sativa L.). *Carbohydrate Polymers, 53*(4), 401-408.

Rieder, A., Grimmer, S., Kolset, S. O., Michaelsen, T. E., & Knutsen, S. H. (2011). Cereal beta-glucan preparations of different weight average molecular weights induce variable cytokine secretion in human intestinal epithelial cell lines. *Food Chem, 128*(4), 1037-1043.

Rieder, A., Knutsen, S. H., & Ballance, S. (2017). In vitro digestion of beta-glucan rich cereal products results in extracts with physicochemical and rheological behavior like pure beta-glucan solutions - A basis for increased understanding of in vivo effects. *Food Hydrocolloids, 67*, 74-84.

Saulnier, L., Gévaudan, S., & Thibault, J. F. (1994). Extraction and Partial Characterisation of β-glucan from the Endosperms of two Barley Cultivars. *Journal of Cereal Science, 19*(2), 171–178.

Sikora, P., Tosh, S. M., Brummer, Y., & Olsson, O. (2013). Identification of high beta-glucan oat lines and localization and chemical characterization of their seed kernel beta-glucans. *Food Chem, 137*(1-4), 83-91.

Singhal, P., & Kaushik, G. (2016). Therapeutic Effect of Cereal Grains: A Review. *Critical Reviews in Food Science and Nutrition, 56*(5), 748-759.

Skau-Mikkelsen, M., Jespersen, B. M., Mehlsen, A., Engelsen, S. B., & Frokiaer, H. (2014). Cereal beta-glucan immune modulating activity depends on the polymer fine structure. *Food Research International, 62*, 829-836.

Storsley, J. M., Izydorczyk, M. S., You, S., Biliaderis, C. G., & Rossnagel, B. (2003). Structure and physicochemical properties of β-glucans and arabinoxylans isolated from hull-less barley. *Food Hydrocolloids, 17*(6), 831-844.

Sullivan, P., O'Flaherty, J., Brunton, N., Gee, V. L., Arendt, E., & Gallagher, E. (2009). Chemical composition and microstructure of milled barley fractions. *European Food Research and Technology, 230*(4), 579-595.

Tosh, S. M. (2013). Review of human studies investigating the post-prandial blood-glucose lowering ability of oat and barley food products. *Eur J Clin Nutr, 67*(4), 310-317.

Tosh, S. M., Wood, P. J., Wang, Q., & Weisz, J. (2004). Structural characteristics and rheological properties of partially hydrolyzed oat β-glucan: the effects of molecular weight and hydrolysis method. *Carbohydrate Polymers, 55*(4), 425-436.

Tvaroska, I., Ogawa, K., Deslandes, Y., & Marchessault, R. H. (1983). Crystalline conformation and structure of lichenan and barley β-glucan. *Canadian Journal of Chemistry, 61*(7), 1608-1616.

Wang, Q., Sheng, X., Shi, A., Hu, H., Yang, Y., Liu, L., Fei, L., & Liu, H. (2017). β-Glucans: Relationships between Modification, Conformation and Functional Activities. *Molecules, 22*(2), 257.

Wood, P. J. (2007). Cereal beta-glucans in diet and health. *Journal of Cereal Science, 46*(3), 230-238.

Wu, J., Zhang, Y., Wang, L., Xie, B., Wang, H., & Deng, S. (2006). Visualization of Single and Aggregated Hulless Oat (Avena nuda L.) (1→3),(1→4)-β -d-Glucan Molecules by Atomic Force Microscopy and Confocal Scanning Laser Microscopy. *Journal of Agricultural and Food Chemistry, 54*(3), 925-934.

Yu, K., Zhou, H. M., Zhu, K. X., Guo, X. N., & Peng, W. (2019). Increasing the physicochemical stability of stored green tea noodles: Analysis of the quality and chemical components. *Food Chem, 278*, 333-341.

Zamora, F., González, M. C., Dueñas, M. T., Irastorza, A., Velasco, S., & Ibarburu, I. (2002). Thermodegradation and thermal transitions of an exopolysaccharide produced by Pediococcus damnosus 2.6. *Journal of Macromolecular Science, Part B, 41*(3), 473-486.

Zhang, L., Li, X., Xu, X., & Zeng, F. (2005). Correlation between antitumor activity, molecular weight, and conformation of lentinan. *Carbohydrate Research, 340*(8), 1515-1521.

Zhu, F. M., Du, B., & Xu, B. J. (2016). A critical review on production and industrial applications of beta-glucans. *Food Hydrocolloids, 52*, 275-288.

Zielke, C., Kosik, O., Ainalem, M. L., Lovegrove, A., Stradner, A., & Nilsson, L. (2017). Characterization of cereal beta-glucan extracts from oat and barley and quantification of proteinaceous matter. *PLoS One, 12*(2).

Zielke, C., Lu, Y., & Nilsson, L. (2019). Aggregation and microstructure of cereal β-glucan and its association with other biomolecules. *Colloids and Surfaces A: Physicochemical and Engineering Aspects, 560*, 402-409.

Highlights

Established a new method assisted by high speed centrifugal-vortex (HSCV) to accelerate the extraction of BBG.

HSCV method reduced the extraction time by half and increased the yield by about 10%.

Extracting history and exogenous physical treatment affected the physicochemical behavior of BBG.

The exogenous physical treatment did not change the primary structure but changed the intermolecular aggregation state of the BBG molecules.

Intermolecular aggregation states and high-level structure of BBG were the noticeable factors influence BBG's solution behavior.